

INVITED PAPER

PACS numbers: 78.67.-n; 42.65.-k; 07.79.-v
DOI: 10.1070/QE2001v031n02ABEH001907

Nanostructures in laser experiments

V S Zuev, A V Frantsesson

***Abstract*. The results of experiments devoted to the excitation of fluorescence and Raman scattering in matter near a nanotip are analysed. The possibilities of practical application of nanotip-enhanced radiative effects are discussed. A brief introduction to the principles underlying the operation of various microscopes with a scanning tip is presented.**

Keywords: *stimulated Raman scattering, nanostructures, tunnelling microscope*.

Recent achievements of laser physics and nonlinear optics are largely due to the use of new active and nonlinear optical materials. Not so long ago, such materials were 'designed' of atoms and molecules in the form of homogeneous crystals, glasses, polymers, and liquid and gas mixtures. An alternative direction, which appeared in recent years, involves the creation of materials with structured bulk characteristics. Macroscopic properties of such materials can be modified in a desirable way by replacing the architecture of microscale structures with an architecture of nanoscale structures. Structured materials with local inhomogeneities much smaller than the wavelength λ of incident radiation then behave as uniform materials with new macroscopic properties.

Generation of the second harmonic of laser radiation ($\lambda = 1064$ nm) on the surface of a plate made of a structured GaP single crystal was observed in experiments [1]. The intensity of the second harmonic in these experiments was increased by a factor exceeding 100 for an electrochemically etched GaP plate with ~ 50-nm pores under conditions when the porosity of the material was equal to 30 %. In spite of the existence of microinhomogeneities (or, to be more precise, nanoinhomogeneities), the plate remained transparent for the visible light. Electrochemically etched pores (produced chaotically) in GaP changed the effective symmetry of the crystal, transforming a system with an initial cubic symmetry into a uniaxially trigonal system. As a result, an optical anisotropy appeared in a GaP crystal, allowing fundamental radiation and its second harmonic to be phase-matched and efficient second-harmonic generation to be observed.

A two-dimensional structure consisting of parallel rods, with their ends resting on a plane, was examined in Ref. [2]. These rods (termed micropillars by the authors) had a diameter of 0.3 – 2.0 μm and a height of 1.15 – 7.75 μm and formed a honeycomb uniform structure. Each rod consisted of a light-emitting GaInAsP/InP heterostructure. Such a structure was shown to permit the enhancement of light emission from a semiconductor with a very high refractive index ($n = 3.38$ at $\lambda = 1.5$ μm). The emission efficiency in these experiments was increased from 2.4 up to 22 – 41 %, since a semiconductor was 'diluted' with voids between the rods, which lowered the effective refractive index. The authors of Ref. [2] also expected that photonic-crystal effect (see below) can be observed with their approach, but this effect was rather weak in these experiments.

Experiments with a structured medium consisting of rods and conducting rings with slits, which possessed properties of a medium with a negative refractive index for wavelengths exceeding the sizes of structure inhomogeneities in the medium are described in Ref. [3]. Natural materials with such properties are not known. The phase velocity of an electromagnetic wave in such an artificial medium has a direction opposite of the direction of the energy flux.

Surface-enhanced Raman scattering (SERS) has been intensely studied and applied in practice since the late 1970s. A rough surface of a highly reflective metal (Au, Ag, Cu, Al) also increases the intensity of other radiative processes, including photoexcited fluorescence, conversion into the second harmonic, etc., which will be called SE effects for brevity below. A clear idea of these studies and interpretation of the relevant experimental results can be gained from paper [4] and references therein.

A rough surface is yet another example of a nanostructured material. The current state of art in this area is described in the literature cited in the papers discussed below in this review. It is important, in our opinion, to include also the paper [5], which presents the results of experiments performed with 100-μm radiation, into this list.

Recently, much attention has been also focused on SE effects due to isolated inhomogeneities having the form of nanorods, sharp needles, and spheres. These studies have shown that signals from isolated inhomogeneities are not only distinguishable against noise, but are also stable and reliable (with a stability better than that attainable with a rough surface). In such experiments, one deals with the observation of radiative effects in atoms and molecules

V S Zuev P N Lebedev Physics Institute, Russian Academy of Sciences, Leninsky prosp. 53, 119991 Moscow, Russia;
e-mail: zuev@sci.lebedev.ru;
A V Frantsesson Institute of Radio Engineering and Electronics, Fryazino Branch, Russian Academy of Sciences, pl. akad. Vvedenskogo 1, 141120 Fryazino, Moscow oblast, Russia

Received 11 October 2000
Kvantovaya Elektronika **31** (2) 120 – 126 (2001)
Translated by A M Zheltikov

located near a very thin tip. It would be no exaggeration to say that tips used in such experiments have a single atom on their ends.

Emission of atoms and molecules near material bodies has recently been a subject of numerous special studies. In this context, we should mention monographs [6, 7], devoted to this problem, and the pioneering work [8]. The formulas predicting the increase in the spontaneous decay rate of an atom in a single-mode waveguide can be found in Refs. [6, 7]. We should note, however, that papers [6–8] are mainly concentrated on the deceleration of the spontaneous decay of atoms. A concept of a photonic crystal, i.e., a crystal with a photonic band gap [8], was proposed as a result of these studies. We, on the other hand, will be interested in the enhancement of spontaneous decay of atoms (molecules). The work by Purcell [9] is, from our point of view, of priority character in this area.

Purcell [9] considered the increase in the rate of spontaneous radiative decay of a quantum object in the case of a nuclear magnetic moment spontaneously emitting radiation near a small metal sphere with a radius $a \ll \lambda$. The rate of spontaneous emission was shown to increase near a small sphere as compared with the emission rate of the same magnetic moment in the space without a sphere or far from such a sphere. The factor characterising the increase in the spontaneous emission rate is given, in accordance with [9], by $f = (\lambda/a)^3$. If $\lambda = 3 \times 10^3$ cm ($\nu = 10^7$ s^{-1}) and $a = 10^{-3}$ cm, then the factor $f = (\lambda/a)^3$ exceeds 10^{19}, and the radiative lifetime of the magnetic moment decreases from 5×10^{21} s down to several minutes. Within the optical range, the ratio λ/a may be equal to 50 ($\lambda = 500$ nm and $a = 10$ nm). The factor f would be $\sim 10^5$ under these conditions.

Investigations of SE effects are closely related to physical processes occurring in microscopes with a scanning tip. In this context, we will briefly consider devices with nanotips and examine the principles underlying the operation of such devices. This class of devices includes scanning microscopes, such as a scanning tunnelling microscope (STM), an atomic-force microscope (AFM), and a scanning near-field optical microscope (SNOM). Without going into the details of operation of these microscopes and the factors leading to their unique spatial resolution, we will mainly focus our attention on the problem of electromagnetic-field enhancement and the increase in the intensity of radiative processes near the tips of such devices.

All the scanning microscopes with a tip are equipped with a unit for a high-precision translation of the probe (instrument) in three coordinates. Such devices (drivers) translate objects by a distance of 10–100 nm with a step of 0.1 nm = 10^{-8} cm and less and a high reproducibility. A tripod with piezoceramic elements (Fig. 1a) or a piezoceramic-tube unit (Fig. 1b) may serve as such a driver. A piezoeffect in ceramics is employed to translate an object in both cases.

Tips for STMs are usually fabricated of tungsten by means of electrochemical etching. Fig. 2 presents an electronic-microscope image of a stainless-steel tip fabricated with the use of an alternative technology – by grinding with a diamond circular grinder.

The design of an STM is shown in Fig. 1a. A tungsten metal tip is fixed in the vertex of a tripod. The tip is located at a distance less than 1 nm from a conducting surface (an object). A voltage of about 1 V is applied to the gap between the tip and the surface. The current flowing through this

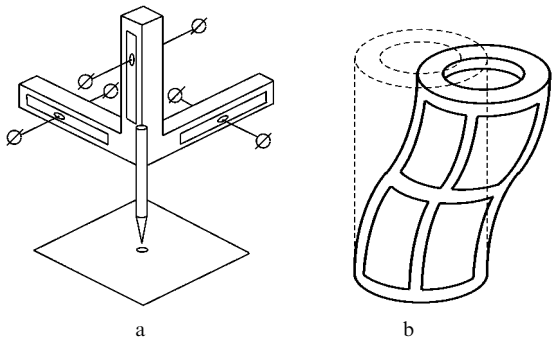

Figure 1. Piezoelectric devices for high-precision three-coordinate translation: (a) a tripod with a tip in its vertex and (b) a piezotube (the solid line shows the displacement of the tube).

Figure 2. A stainless-steel STM tip.

circuit is equal to $\sim 10^{-9}$ A. The current arising due to the tunnelling of electrons through the tip–surface gap strongly (exponentially) depends on the width of this gap. If the conducting surface has a relief, then this relief is visualised in the case of two-coordinate scanning from the variation in the tunnelling current or from the longitudinal displacement of the tip required to sustain the tunnelling current constant. The spatial resolution attainable with such an approach may be as high as fractions of a nanometer. The tunnelling of electrons is also employed in other scanning microscopes.

Tips for an AFM are fabricated by means of photolithography – by etching Si or SiN crystals. The choice of the material for tips is dictated by the fabrication process, since the etching rate of the surface of a single crystal depends on the orientation of the surface with respect to the symmetry axes of a single crystal. The etching rate may be higher for some crystallographic directions and lower for other crystallographic directions. This circumstance allows micropyramids with extremely sharp tops to be fabricated. Such a pyramid may serve as a tip in an atomic-force microscope (Fig. 3). The height and the diameter of the tip base in this case fall within the range of 10 – 15 μm. A longitudinal shift of the tip gives rise to a detectable deformation of a lever.

A tip, which is located adjacent to the surface of a solid, is subject to the action of molecular (atomic) repulsion forces, arising due to the Pauli exclusion principle for electrons, and of long-range van der Waals forces, which are less significant in the case under consideration. The surface relief of repulsion forces is nonuniform even in the case of an atomically smooth surface. An AFM allows monoatomic growth layers, quantum dots, and other objects to be observed.

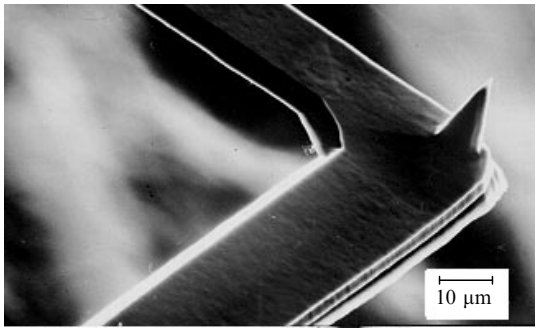

Figure 3. An AFM tip on a V-shaped spring lever.

Currently, AFMs employ a U-shaped piezoquartz tuning fork with a tip attached to its tine. The tuning fork is equipped with electrodes, which are employed to drive mechanical vibrations of the tine with a tip. The amplitude of these vibrations does not exceed 0.1 nm. The tip is subject to friction at the atomic–molecular level near a sample surface, which decreases the amplitude of mechanical vibrations. This change in the vibration amplitude is detected using the inverse piezoeffect. In the case of two-dimensional scanning, a surface relief can be detected with an atomic-scale resolution.

Finally, consider the principle underlying the operation of a scanning near-field optical microscope. Before proceeding with this analysis, we discuss the problem of minimal spatial features in an electromagnetic field. Features with sizes less than $\lambda = 2\pi/k$ ($k = \omega/c$ is the wave number) are absent in optical images, interferograms, and holograms. The scale of spatial features is determined by projections of the wave vector $\boldsymbol{k}$ on the relevant axes. The equality

$$k^2 = k_x^2 + k_y^2 + k_z^2 = (2\pi/\lambda)^2. \tag{1}$$

should be satisfied for these projections. Since $k_i^2 \leqslant k^2$ in this inequality, all the field features should have spatial sizes no less than $n\lambda$ ($n = 0.3 - 0.5$). In our analysis, we will assume that $n = 1$ for simplicity.

The situation radically changes when the so-called inhomogeneous waves of the form $f(x, y, z) \sim \exp(-k_x x) \times \exp(\mathrm{i}k_z z)$, $k_y = 0$ appear among the spatial harmonics of the field. An inhomogeneous wave is defined as a wave where the constant-amplitude plane differs from the constant-phase plane. The wave arising on the surface of a prism of total internal reflection may serve as an example of an inhomogeneous wave. The field exponentially decreases in a medium with a lower refractive index with the growth of the distance from an interface between two media with different refractive indices along the normal to this interface. This implies that one of the components is purely imaginary, and, consequently, the square of this component is negative. Therefore, setting $k_y^2 = 0$ and $k_z^2 < 0$ in Eqn (1) for definiteness (the z axis is perpendicular to the interface), we find that $k_x^2 > k^2 > 0$. Thus, inhomogeneous electromagnetic waves may produce features with inhomogeneities of sizes less and even much less than the wavelength λ.

As an example of such a feature, we can consider the field of an oscillating elementary electric dipole $\boldsymbol{p} = \boldsymbol{p}_0 \exp(-\mathrm{i}\omega t)$. If we represent this field in the form of a plane-wave expansion, inhomogeneous waves inevitably arise in this field. We do not present this expansion because of its cumbersome form, providing only expressions for the field of a dipole in the form of spherical waves:

$$E_r = \frac{p_0}{2\pi\varepsilon}\cos\theta\left(\frac{1}{r^3} - \frac{\mathrm{i}k}{r^2}\right)\exp[-\mathrm{i}(\omega t - kr)],$$

$$E_\theta = \frac{p_0}{4\pi\varepsilon}\sin\theta\left(\frac{1}{r^3} - \frac{\mathrm{i}k}{r^2} - \frac{k^2}{r}\right)\exp[-\mathrm{i}(\omega t - kr)], \tag{2}$$

$$H_\varphi = -\mathrm{i}\frac{\omega p_0}{4\pi}\sin\theta\left(\frac{1}{r^2} - \frac{\mathrm{i}k}{r}\right)\exp[-\mathrm{i}(\omega t - kr)].$$

At large distances from a dipole ($kr \gg 1$), the field has a conventional structure of a spherical wave with the distances between the field maxima equal to λ. However, due to the presence of the terms proportional to r^{-2} and r^{-3}, the field noticeably changes near the dipole ($kr \ll 1$) for the distances much less than λ.

Scanning near-field optical microscopy is based on the use of a light source in the form of a small (~ 50 nm) hole in an opaque screen. The electromagnetic field behind this hole in a conducting screen is equivalent to the field induced by a combination of electric and magnetic elementary dipoles [10, 11]. Obviously, metals have different dielectric properties within the microwave and optical frequency ranges. Within the microwave range, we have $\varepsilon \simeq \mathrm{i}\varepsilon''$, with $\varepsilon'' \gg 1$. Within the optical range, we arrive at $\varepsilon = -\varepsilon'$, with $\varepsilon' \gg 1$. However, writing the boundary conditions in the form of the so-called Leontovich condition [12] for the tangential components of the field,

$$\boldsymbol{E}_\mathrm{t} = \left(\frac{\mu}{\varepsilon}\right)^{1/2}[\boldsymbol{H}_\mathrm{t}\boldsymbol{n}], \tag{3}$$

where $\boldsymbol{n}$ is the normal to the interface between two media, to $R|\varepsilon| \gg 1$ we find no difference between the boundary conditions for metals within the microwave and optical frequency ranges (within some approximation): $\boldsymbol{E}_\mathrm{t} = 0$ in both cases. With $\omega \neq 0$ and $\boldsymbol{E}_\mathrm{t} = 0$, the boundary condition $H_\mathrm{n} = 0$ automatically follows from the Maxwell equation $\mathrm{rot}\,\boldsymbol{E} = (\mathrm{i}\omega/c)\boldsymbol{H}$.

The conditions $\boldsymbol{E}_\mathrm{t} = 0$ and $\boldsymbol{H}_\mathrm{n} = 0$ remain (approximately) the same for problems with both ideal conductors and ideally reflecting metals, which implies that the results of microwave theory can be employed in optical problems. The Leontovich condition remains applicable as long as the penetration depth of the field in a metal ($\sim 10^{-6}$ cm) remains less than the curvature radius of the surface [12].

If a thin-film object is located between a light source and a detector (adjacent to the light source), then the structure of this nonuniform object can be detected by scanning the object with a spatial resolution equal to the diameter of the hole. It is appropriate to choose the minimum diameter of the hole equal to twice the thickness of the skin layer in a metal, which corresponds to ~ 10 nm.

A small hole can be also employed as a detector. In practice, a movable probe (a source or a detector) has a form of a pipette with a very small diameter made of a dielectric fibre tapered by drawing the fibre until it is disrupted under conditions of local heating. Next, an aluminium coating is deposited on the dielectric tip in such a way that the

vertex of the tip remains uncoated. The distance between the probe and an object in a scanning optical microscope is determined either from the tunnelling current, similar to an STM, or from the friction force, similar to an AFM. In certain cases (e.g., when the inhomogeneous wave is excited on a prism of total internal reflection), the distance between the probe and the object is determined from the amplitude of the optical signal.

A metal micropipette (or, to be more specific, nanopipette) probe possesses a very low transmittance: light is attenuated by a factor of $10^5 - 10^6$ in such a probe. This attenuation is of waveguide nature. The problem is that a metal waveguide with a cross section diameter less than the radiation wavelength does not support propagating waves [12]. The field may only enter a waveguide, exponentially decreasing along the waveguide length.

Recently, an optical probe with three sequential conical surfaces coaxial with an optical fibre has been implemented [13]. The first two surfaces concentrate light on the input of the last cone, which has a small diameter and a small length. This approach allowed the transmittance of an optical probe to be increased by a factor of about 1000. The length of the narrowest part in such a probe is very small, permitting the losses of an optical signal to be considerably reduced.

The highest spatial resolution (0.8 nm) can be achieved with the so-called apertureless SNOM [14], where a semiconductor tip with no metal coating is used. The vertex of such a tip scatters incident radiation and serves as a source of light with an extremely small diameter. The tip emits a dipole electric wave (see the Mie theory for the scattering of light from a small sphere [12]). This device provides a remarkably high resolution, but is characterised, at the same time, by a very sophisticated design due to the necessity of taking special precautions to attenuate background radiation.

The capability of probes to transmit electromagnetic radiation can be radically enhanced by placing a conical metal tip on the axis of a metal pipette. This new device has a form of a conical coaxial line – a bicone (Fig. 4).

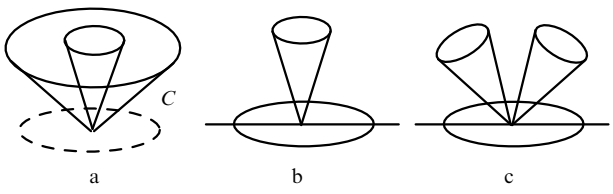

Figure 4. Different types of bicones.

As is well known from the microwave theory, a bicone supports the so-called fundamental wave with zero critical frequency ω_{cr} [15]. The condition $\omega_{cr} = 0$ implies that an ideally conducting bicone may have an arbitrarily small cross section.

We have shown (see Ref. [16] and references therein) that a bicone with a small cross section made of a highly reflective metal may operate at optical frequencies. Fig. 4a shows a bicone formed by two conical surfaces, with apex angles of each of the cones being less than π. The bicone shown in Fig. 4b has a much simpler design. This bicone consists of a conical tip and a plane. The plane can be considered as a cone with an apex angle equal to π. Fig. 4c shows a bicone in the form of two tips. The resulting conical wire line also supports the fundamental wave with the critical frequency $\omega_{cr} = 0$.

Analysis of Fig. 4a shows that the circulation of the magnetic field along a circular contour C coaxial to the bicone near its vertex in the plane perpendicular to the bicone axis is equal to zero. Two counterpropagating currents with equal magnitudes (in the outer and inner conducting cones) go through this countour. Therefore, the minimum appropriate diameter of the output cross section of the bicone is no longer determined by the thickness of the skin layer, as it was in the case of a metal pipette. This statement can be easily verified for a bicone made of an ideally conducting metal. Within the optical frequency range, analysis becomes rather complicated. We plan to test this property of a bicone experimentally.

Now, let us discuss experiments performed with scanning microscopes employing tips with extremely sharp vertices. Proceeding with this analysis, we are mainly interested not in the spatial resolution of the scanning microscope, but rather in phenomena that occur in matter near the tip vertex. In certain cases, these phenomena have much in common with processes observed on a rough surface of a highly reflective metal (Au, Ag). In the latter case, an isolated element of a rough metal surface is equivalent to a tip.

The ideas of experiments proposed in Refs [17, 18] are based on the concepts of the electrostatic theory of tips. However, these experiments, in fact, demonstrate the focusing effect of an optical bicone having a form of a metal tip and a metal plane.

The study [17] is devoted to effects accompanying the interaction between a tip end and a metal surface in the regime when an STM tip is irradiated by 532-nm pulses of focused laser radiation. For an energy flux density of 5-ns laser radiation pulses in a light spot of 10^7 W cm^{-2} and higher, hills or grooves with diameters of 30 – 50 nm are produced on a plane surface. The results of these experiments depended on the relative refractory ability of the tip and the surface (Ag, W, Pt, etc.). In our opinion, experiments [17] have demonstrated the subwavelength focusing of laser radiation near the vertex of a bicone, i.e., on the tip of a probe with a diameter of approximately 100 nm.

The intensification of laser radiation in an STM gap between a platinum tip and a conducting surface was also studied in Ref. [18]. The plane surface in these experiments was made either of a highly oriented pyrolytic graphite or gold. The dc component of the photocurrent through the gap between a tip and a conducting surface was measured in these experiments. These measurements gave grounds to assume [18] that the optical field around the tip vertex is intensified more than by a factor of 1000 as compared with the field intensity in a laser beam. Unfortunately, no explicit expression for the intensification factor is presented in [18], which prevents one from understanding whether this factor corresponds to the ratio of field intensities or field strengths.

The considered effect was interpreted in Ref. [18] in terms of the electrostatic theory of a conducting tip (see, e.g., [12]). In our opinion, the results of Ref. [18] provide yet another experimental demonstration of the excitation of a converging wave in an optical coaxial line (an optical bicone) and subwavelength focusing of laser radiation.

In STM experiments [19], the gap between a metal tip and a metal plane surface was excited with an electromagnetic field of a surface plasmon. These experiments have

demonstrated that the power consumed from the plasmon wave increases when the tip is located at a small distance (< 1 nm) from the surface. This finding was interpreted in terms of the antenna effect of the tip. In other words, this experiment demonstrates the excitation of a diverging fundamental wave, i.e., the wave with a zero critical frequency in an optical bicone.

It is of considerable interest to discuss SE effects observed in matter near the vertex of a sharp tip. Under certain conditions, these effects are reminiscent of the phenomena occurring on a rough surface of a highly reflective metal. SE effects may be associated either with the properties of the electromagnetic field or with phenomena of some other nature, e.g., chemical processes. Below, we will consider effects related to the electromagnetic field.

The first effect is called the antenna effect. A local elevation on a metal surface may serve as a receiving or transmitting (emitting) antenna. The influence of the antenna effect can be assessed with the use of formulas from the Mie theory of plane-wave scattering from a sphere (see, e.g., [20]). The intensity of the total field (the incident wave + the scattered wave) increases by a factor of approximately 12 near a conducting sphere with a diameter of $\sim \lambda$. The sphere in this situation serves as a receiving antenna.

An elementary electric dipole placed near a conducting sphere, whose diameter is approximately equal to λ, emits radiation with an intensity approximately 20 times higher than the intensity of radiation emitted by the same dipole in free space. In this case, the sphere serves as an emitting antenna. The above estimate was made in the dipole approximation using formulas similar to the formulas of the Mie theory. A plane incident wave in these calculations was replaced by an electric-dipole diverging wave [21].

The second phenomenon is called the lightning-rod effect. Our understanding is that this term stems from the light emitted by the ends of sharp metal objects during a thunder (St. Elmo's fire). This emission is caused by the increase in the field intensity near a tip. This effect can be easily calculated for an ellipsoid of revolution whose size is much less than λ. The values of ε and μ at the relevant frequency should be inserted into the electrostatic formulas to perform such a calculation [12]. The field on the tip of a prolate ellipsoid can be calculated from the formula

$$E_{\text{tip}} = \frac{(1 - A_{\text{a}})(\varepsilon - 1)}{1 + (\varepsilon - 1)A_{\text{a}}} E_{\text{L}} + E_{\text{L}}, \tag{4}$$

where E_{L} is the field of the incident wave; $A_{\text{a}} = 1/3$ for a sphere; $A_{\text{a}} \ll 1$ in the case of a strongly prolate ellipsoid. For $(\varepsilon - 1)^{-1} \ll A_{\text{a}}$, we have $E_{\text{tip}} = (1/A_{\text{a}} + 1)E_{\text{L}}$, while for $(\varepsilon - 1)^{-1} \gg A_{\text{a}}$, the field is given by $E_{\text{tip}} = \varepsilon E_{\text{L}}$. In both cases, the field intensity near an ellipsoid is higher than the field intensity near a sphere.

The third effect is called plasmon resonance. A plasmon is an eigenmode of the electron (electron plasma) motion in a metal. The motion of electrons induces an electromagnetic field. A plasmon resonance is seen from the Mie-theory formula for the scattering of an electromagnetic wave by a small sphere with a radius $a \ll \lambda$ [12, 20]:

$$\mathscr{E} \simeq -\frac{2\mathrm{i}}{3}\frac{\varepsilon - 1}{\varepsilon + 2}(ka)^3 E_0, \tag{5}$$

where $\mathscr{E}$ is the amplitude of the scattered (electric-dipole) wave. The dielectric constant ε in this case is negative and frequency-dependent. Within a certain frequency range in the visible spectral region, $\varepsilon = -2 + \mathrm{i}\varepsilon''$, $\varepsilon'' \ll 1$, for Au and Ag. The amplitude $\mathscr{E}$ may become very large in this range (increasing by a factor of 10^4 and more [22]). This phenomenon is called a plasmon resonance. The term 2 in the denominator of Eqn (5) depends on the shape of a particle, being larger for an ellipsoid, and the frequency of the plasmon resonance is lower (ε increases in its absolute value with the lowering of the frequency).

The fourth effect is the Purcell effect [9], which involves the increase in the rate of spontaneous emission near a small sphere relative to the spontaneous emission rate in a space without a sphere or far from such a sphere.

Let us discuss now the most recent studies performed in the field under consideration (published in the spring of 2000). A suspension of gold nanorods, i.e., a set of tips, was employed in experiments [23] instead of an isolated tip. The diameter of these rods was ~ 20 nm, while their lengths ranged from 40 to 108 nm. One can see from a microimage presented in Ref. [23] that nanorods are distributed in the bulk of suspension within distances of the order of their length.

Fluorescence of Au nanorods excited by light at 480 nm was observed in the wavelength range from 548 to 590 nm. These nanorods allowed the fluorescence intensity to be increased by a factor of $10^{-6} - 10^{-7}$ as compared to the fluorescence yield of a solid Au surface.

The authors of paper [24] observed Raman scattering of light by BCB (brilliant cresyl blue) and C_{60} molecules deposited on the surface of glass as a thin layer. A sharp metal tip was brought in contact with (or adjacent to) the surface of this molecular film. A SiN tip coated with a thin silver layer with a vertex rounding diameter of less than 50 nm was used in the former case, and a gold tip with a vertex rounding diameter of less than 20 nm was employed in the latter case. A considerable increase in the intensity of Raman scattering (by a factor of 30 for BCB molecules and by a factor of 40 for C_{60} molecules) was observed when the tip was brought in contact with a molecular film under study.

Taking into account the ratio of the diameter of the laser beam to the diameter of the tip vertex, authors found that the intensity was increased by a factor of 2000 in the case of BCB molecules and by a factor of 40000 in the case of C_{60} molecules. A SiN tip with no silver coating did not increase the signal of Raman scattering. Note (with reference to [24]) that, in the case of C_{60} molecules, they deal not only with the effect of the electromagnetic field, but also with a chemical effect, which is related to charge transfer due to the contact potential difference. This chemical effect gave rise to new lines in the Raman spectrum.

Our understanding is that a SiN tip without a metal coating should also influence the intensity of Raman scattering, but this effect should be weaker than in the case of a metal tip. The influence of a Si tip on Raman scattering was observed in experiments described in Ref. [25], where the fluorescence of a small dyed dielectric sphere was studied near the tip of an apertureless near-field optical microscope. A Si tip with a vertex rounding radius of about 5 nm was placed adjacent to a polystyrene sphere with a diameter of 45 nm in these experiments. Analysis of the results of these experiments gave grounds to conclude that a tip gives a more than 100-fold increase in the intensity of pump radiation.

In Ref. [26], Raman scattering was observed on the surface of a sulphur film (produced by settling sulphur on

the surface from an acetone solution) near a gold tip with a vertex rounding diameter of 45 nm. An Au-coated Si tip from an AFM was used in experiments [26]. No Raman scattering signal was detected in the absence of a tip. The use of a tip allowed Raman scattering to be detected with a reasonable signal-to-noise ratio. According to the estimates of [26], the enhancement factor of Raman scattering under these conditions exceeded 10^4.

In conclusion, we will present the results of the study [27], where an STM tip was employed to initiate the reaction

$$2C_6H_5I \xrightarrow{Cu} C_{12}H_{10} + I_2$$

between two isolated (selected with an STM tip) C_6H_5I molecules. This reaction is catalysed by copper. These experiments were performed on a pure copper surface with an atomic step distinguishable by an STM. Two adjacent C_6H_5I molecules attached to the atomic step were selected by an STM tip. The STM tip was aimed sequentially at each of these molecules. When the molecule was localised, the voltage applied to the tip was increased up to 1.5 V. An I atom under these conditions was detached due to the tunnelling of electrons. The energy of these electrons was sufficient to break the C–I bond, but insufficient to break C–C and C–H bonds. The same operation was repeated for each of the C_6H_5I molecules. Free iodine atoms were removed from the reaction area sideways with the use of the tunnelling tip. Then, this tip was employed to bring the radicals closer to each other by transferring them along the atomic step.

However, no dimerisation reaction was observed when the radicals were brought closer to each other, and it was possible to separate C_6H_5 radicals. Then, these radicals were brought into a contact again, an the voltage applied to the tunnelling tip was increased up to 0.5 V. Under these conditions, C_6H_5 radicals turned their valence bonds toward each other. Steric difficulties were eliminated, and the radicals united into a single $C_{12}H_{10}$ molecule. This process was confirmed by the fact that the new formation moved as a single unit, without decaying into two parts. Similar excitations can be also implemented, in our opinion, with the use of photons.

In conclusion, we should note that experiments that have demonstrated a considerable increase in the intensity of the Raman scattering signal or the fluorescence signal in matter near a metal or semiconductor tip seem to be of fundamental importance from both physical and practical viewpoints. The results of these experiments can be employed to develop clear theoretical models and then to determine the physical mechanisms and the nature of surface-enhanced radiative processes. We expect that new important results will be obtained in this area in the nearest future.

On the other hand, the results of these experiments, regardless of their theoretical interpretation, offer much promise for many interesting applications. Here, we will mention only two of them. The first application is associated with the analysis of materials, including the analysis of extremely low amounts of matter (hundreds of molecules in a sample) through the spectroscopy of Raman and hyper-Raman scattering or fluorescence spectroscopy. The idea of observing the spectra of Raman and hyper-Raman scattering was proposed by V S Gorelik through a communication with the authors of this paper. Later, we found the mentioning of this idea in Ref. [26]. It is anticipated that both AFMs and the equipment for the detection of Raman scattering will be employed during the Mars mission (2001 Mars Surveyor NASA project). Such devices may provide an opportunity to analyse extremely low amounts of matter in samples.

The second important application may be associated, in our opinion, with the creation of an ultrahigh-capacity data-storage system. An authorship of this proposal belongs to us unless predecessors will be found. Suppose that a tip, i.e., a device of the atomic-scale spatial resolution to be achieved, is placed adjacent to a crystal surface. Separate molecules (or atoms) at the sites of the crystal lattice can be distinguished with such a tip. The state of a molecule can be changed in one way or another.

Let us assume that there are two states of a molecule with different Raman spectra. Changing the state of a molecule, we can write the bits 0 and 1 using a single molecule for data storage. A molecule in state 1 may then correspond to the bit 0, while a molecule in state 2 with different Raman spectrum may correspond to the bit 1.

An effect of a sharp tip is used to write (or read) the data. The Raman spectrum appears only when the tip vertex is brought in the vicinity of the relevant molecule. Let us set the distance between molecules equal to 0.3 nm. The number of molecules on the surface of a crystal may then reach 10^{15} molecules per 1 cm^2. Consequently, 1 cm^2 of a crystal surface may contain 1.25×10^{14} bytes, or 7.8×10^{14} bytes per square inch, which corresponds to approximately 10^6 gigabytes per square inch.

Acknowledgements. The authors thank A V Vinogradov for his interest in this work. This research was partially supported by the Russian Foundation for Basic Research, (Grants Nos 00-02-17459 and 00-02-16655).

References

1. Tiginyanu I M, Kravetsky I V, Monecke J, Cordts W, Marow-sky G, Hartnagel H L *Appl. Phys. Lett.* **77** 2415 (2000)
2. Baba T, Inoshita K, Tanaka H, Yonekura J, Ariga M, Matsu-tani A, Miyamoto T, Koyama F, Iga K J. *Lightwave Technol.* **17** 2113 (1999)
3. Smith D R, Padilla W, Vier D C, Nemat-Nasser S C, Schultz S *Phys. Rev. Lett* **84** 4184 (2000)
4. Boyd G T, Raising Th, Leite J R R, Shen Y R *Phys. Rev. B* **30** 519 (1984)
5. Shulman A Ya *Phys. Status Solidi (a)* **175** 279 (1999)
6. Bykov V P, Shepelev G V *Izluchenie Atomov vblizi Material'-nykh Tel* (Emission of Atoms near Material Bodies) (Moscow: Nauka, 1986)
7. Bykov V P *Radiation of Atoms in a Resonant Environment* (Singapore: World Scientific, 1993)
8. Yablonovitch E *Phys. Rev. Lett.* **58** 2059 (1987)
9. Purcell E M *Phys. Rev.* **69** 681 (1946)
10. Bethe H *Phys Rev.* **66** 163 (1944)
11. Bouwkamp C J *Physica* **12** 467 (1946)
12. Landau L D, Lifshitz E M *Elektrodinamika Sploshnykh Sred* (Electrodynamics of Continuous Media) (Moscow: Nauka, 1982)
13. Yatsui T, Kourogi M, Ohtsu M *Appl. Phys. Lett.* **73** 2090 (1998)
14. Martin Y, Zenhausern F, Wickramasinghe H K *Appl. Phys. Lett.* **68** 2475 (1996)
15. Schelkunoff S A *Electromagnetic Waves* (New York: van Nostrand, 1947)
16. Zuev V S, Frantsesson A V *Pis'ma Zh. Eksp. Teor. Fiz.* **72** 115 (2000)

17. Jersch J, Dickmann K *Appl. Phys. Lett.* **68** 868 (1996)
18. Bragas A V, Landi S M, Martinez O E *Appl. Phys. Lett.* **72** 2075 (1998)
19. Specht M, Pedarnig, J D, Heckl W M, Hansch T W *Phys. Rev. Lett.* **68** 476 (1992)
20. Stratton J A *Electromagnetic Theory* (New York: McGraw-Hill, 1941)
21. Ivanov E A *Difraktsiya Elektromagnitnykh Voln na Dvukh Telakh* (Diffraction of Electromagnetic Waves from Two Bodies) (Minsk: Nauka i Tekhnika, 1968)
22. Wokaun A, Gordon J P, Liao P F *Phys. Rev. Lett.* **48** 957 (1982)
23. Mohamed M B, Volkov V, Link S, El-Sayed M A *Chem. Phys. Lett.* **317** 517 (2000)
24. Stockle R M, Suh Y D, Deckert V, Zenobi R *Chem. Phys. Lett.* **318** 131 (2000)
25. Hamann H F, Gallagher A, Nesbitt D J *Appl. Phys. Lett.* **76** 1953 (2000)
26. Anderson M S *Appl. Phys. Lett.* **76** 3130 (2000)
27. Hla S-W, Bartels L, Meyer G, Rieder K-H *Phys. Rev. Lett.* **85** 2777 (2000)